



Association between ribs shape and pulmonary function in patients with Osteogenesis Imperfecta

Juan A. Sanchis-Gimeno^{a,*}, Stephanie Lois-Zloliniski^b, José María González-Ruiz^b, Carlos A. Palancar^b, Nicole Torres-Tamayo^{a,b}, Daniel García-Martínez^b, Luis Aparicio^a, Marcelino Perez-Bermejo^a, Esther Blanco-Perez^{a,c}, Federico Mata-Escolano^d, Susanna Llidó^a, Isabel Torres-Sanchez^e, Francisco García-Río^{e,f}, Markus Bastir^{a,b}

^a Gival Research Group, Department of Anatomy and Human Embryology, Faculty of Medicine, University of Valencia, Av. Blasco Ibañez, 15, 46010 Valencia, Spain

^b Departamento de Paleobiología, Museo Nacional de Ciencias Naturales (CSIC), José Gutiérrez Abascal 2, 28006 Madrid, Spain

^c Department of Radiology, University Hospital de La Ribera, Carretera Corbera Km 1, 46600 Alzira, Valencia, Spain

^d ASCIRES ERESA Campanar Group, CT and MRI Unit, Avda. de Campanar 114, 46015 Valencia, Spain

^e Hospital La Paz Institute for Health Research (IdiPAZ), Paseo de la Castellana 261, 28046 Madrid, Spain

^f Centro de Investigación Biomédica en Red en Enfermedades Respiratorias (CIBERES), Instituto de Salud Carlos III, Calle Monforte de Lemos 3-5, 28029 Madrid, Spain

HIGHLIGHTS

- Chest deformities in Osteogenesis Imperfecta patients affect pulmonary function.
- We present the rib cage deformities related to pulmonary function.
- There are significant relations between ribs shape and spirometric parameters.
- There is no relationship between thoracic spine shape and spirometric parameters.
- Correction of rib cage deformities will serve for better patients' management.

GRAPHICAL ABSTRACT



ARTICLE INFO

Article history:

Received 3 July 2019

Accepted 18 October 2019

Available online 22 October 2019

Keywords:

Geometric morphometrics

Osteogenesis imperfecta

Pulmonary function

Rib cage

Scoliosis

Thoracic spine

ABSTRACT

The aim of the present study was to test the hypothesis that ribs shape changes in patients with OI are more relevant for respiratory function than thoracic spine shape. We used 3D geometric morphometrics to quantify rib cage morphology in OI patients and controls, and to investigate its relationship with forced vital capacity (FVC) and forced expiratory volume in 1 s (FEV1), expressed as absolute value and as percentage of predicted value (% pred). Regression analyses on the full sample showed a significant relation between rib shape and FEV1, FVC and FVC % pred whereas thoracic spine shape was not related to any parameter. Subsequent regression analyses on OI patients confirmed significant relations between dynamic lung volumes and rib shape changes. Lower FVC and FEV1 values are identified in OI patients that present more horizontally aligned ribs, a greater antero-posterior depth due to extreme transverse curve at rib angles and a strong spine invagination, greater asymmetry, and a vertically short, thoracolumbar spine, which is relatively straight in at levels 1–8 and shows a marked kyphosis in the

Peer review under responsibility of Cairo University.

* Corresponding author at: Gival Research Group, Department of Anatomy and Human Embryology, Faculty of Medicine, University of Valencia, Avda. Blasco Ibañez, 15, E46010 Valencia, Spain.

E-mail address: juan.sanchis@uv.es (J.A. Sanchis-Gimeno).

<https://doi.org/10.1016/j.jare.2019.10.007>

2090-1232/© 2019 The Authors. Published by Elsevier B.V. on behalf of Cairo University.

This is an open access article under the CC BY-NC-ND license (<http://creativecommons.org/licenses/by-nc-nd/4.0/>).

thoraco-lumbar transition. Our research seems to support that ribs shape is more relevant for ventilator mechanics in OI patients than the spine shape.

© 2019 The Authors. Published by Elsevier B.V. on behalf of Cairo University. This is an open access article under the CC BY-NC-ND license (<http://creativecommons.org/licenses/by-nc-nd/4.0/>).

Introduction

Osteogenesis Imperfecta (OI) is a rare disease, occurring in 1 per 15,000 to 20,000 births and affecting 1 in every 200,000 individuals, presenting no gender or race predominance [1]. OI is a genetic disorder caused by a qualitative or quantitative defect of Type I collagen – the most abundant protein of the extracellular matrix of bone – mainly driven by autosomal dominant mutations in the genes that code for collagen Type I alpha chains COL1A1 and COL1A2 [2,3], although mutations in more than ten other genes can also lead to OI [3].

The phenotypic expression of OI was originally classified by Silence et al. [4,5] into four clinical types: i.e. Type I, II, III, and IV. Each four clinical types have a different life expectancy, ranging from lethal (Type 2) to similar to the general population (Type I patients), being slightly reduced in Type IV and strongly decreased in Type III [6–8]. OI Type III is the most severe type among those patients who survive the first year of life, leading to a progressive and deforming evolution [9]. Additional types (up to nine types) have been described as knowledge about OI genetics has increased [10].

Previous studies have analyzed the clinical symptoms of OI patients using different methods, concluding that OI patients are characterized by bone fragility, frequent fractures, spine anomalies and rib cage deformities [3–5,11–17]. Nevertheless, it is not completely clear how these features affect the ventilatory mechanics of patients with this disease [7]; it is known, however, that respiratory disease is the principle cause of death in OI patients (81.6% of the deaths in OI Type III, 39% in the Type I and IV and 15.7% in the general population) [6]. The progressive chest deformities presented by OI patients tend to affect pulmonary function [14,17]. LoMauro et al. [14] studied the relationship between the progressive chest deformities and the pulmonary function and they suggested a direct relationship between the structural modifications of the rib cage and the pattern of volume variations during breathing in patients with severe OI. More specifically, these authors suggested that the deformation of the ribs was more important for respiratory function than scoliosis. More recently, LoMauro et al. [17] suggested that the combination of flattened vertebrae, floppy ribs, more horizontal ribs, spinal, and sternal deformity are the causes of the impaired expansion of pulmonary rib cage in severe OI.

However, LoMauro et al. [14,17] analyzed the external chest wall only, while the complex morphology of the internal skeletal thoracic anatomy (i.e. ribs, vertebrae, etc.) is best approached through 3D geometric morphometrics on computed tomography (CT) data [18–21]. To our knowledge, there is not any work quantifying the anatomical relationship between the 3D morphology of

the ribcage and the respiratory function. Therefore, the aims of the present study were to quantitatively test by means of 3D geometric morphometrics if rib shape changes in patients with severe OI are more relevant for respiratory function than thoracic spine shape, and to detect the anatomic configuration related to a worse respiratory function in OI patients.

Methods

Study population

Adult subjects with OI were recruited for this study on a voluntary basis after approval of the research protocol by the local Ethics Committee of the University of Valencia, Spain (approval n. H1417174744011). All OI patients were volunteers from the Fundación AHUCE of Spain. Written informed consent was obtained from each participant. Inclusion criteria were patients diagnosed with OI [17], clinically classified as Type III and Type IV and confirmed by genetic testing. Patients with any other metabolic bone disease except OI and those who underwent surgery for correction of ribcage and/or spinal deformities were excluded. All patients are currently receiving bisphosphonate therapy.

Additionally, as control group, sex-matched non-smoking healthy adults were selected from La Paz Hospital cohort (Madrid, Spain), recruited in previously published studies [19–22]. These subjects were free of any pulmonary or spinal pathology. The study was also approved by their institutional ethics committee (CEI Hospital Universitario La Paz; HULP-PI-513) and each participant gave written informed consent for the use of their medical data.

The final study population (Table 1) consisted of 12 patients with OI (7 females, 5 males; 9 Type III and 3 Type IV) and 12 control subjects (7 females, 5 males).

Pulmonary function tests

Spirometry was performed on all subjects by trained clinicians in accordance with the Spanish Society of Pulmonology and Thoracic Surgery guidelines [23] and equations of the Global Lung Function Initiative 2012 [24] were used as reference values. Individual measures of forced vital capacity (FVC) and forced expiratory volume in 1 s (FEV1), expressed as absolute value and as percentage of predicted value, are shown in Table 2.

CT protocol and imaging evaluation

Two CT scans per subject were carried out in a 15 min interval. The subjects were instructed to hold their breath in the maximal inspiration during the first scan and in the maximal expiration

Table 1
Description of the samples analyzed.

	Osteogenesis Imperfecta		Control sample		p-value*
	Median	IQR**	Median	IQR**	
Age (years)	41.0	30.5–50.75	64.5	61–68.5	<0.001
Body height (cm)	137.5	116.25–167.25	166.0	157.75–175.5	0.006
Body weight (kg)	51.0	39.5–69.0	68.0	59.25–87.25	0.032
Body mass index (kg/m ²)	29.1	23.53–33.15	24.55	23.18–28.13	0.179

* Mann-whitney test.

** IQR: interquartile range.

Table 2

Spirometric values obtained in the subjects analyzed.

	Osteogenesis Imperfecta		Control sample		p-value*
	Median	IQR**	Median	IQR**	
FVC (L)	2.31	1.45–3.19	3.54	3.07–4.84	0.003
FEV1 (L)	2.02	1.35–3.09	2.75	2.53–3.96	0.021
FVC, % pred (%)	81.9	67.8–112.15	121.0	104.3–125.63	0.005
FEV1, % pred (%)	86.85	69.55–128.48	113.9	105.55–122.95	0.073

FVC: forced vital capacity; FEV1: forced expiratory volume in 1 s, FVC% pred: forced vital capacity expressed as percentage of predicted value; FEV1% pred: forced expiratory volume in 1 s expressed as percentage of predicted value.

* Mann-whitney test.

** IQR: interquartile range.

during the second one. The CT scans were post-processed to obtain multiplanar, maximum intensity projection and 3D reconstruction images [25]. Finally, the marching cubes algorithm was applied to obtain 3D virtual models of the ribcages [26].

3D geometric morphometrics analysis and respiratory function

Geometric morphometrics in 3D (3D GM) is defined as the statistical analysis of Cartesian landmark coordinates, which have both, biological meanings and homologous locations on the analysed anatomical structures [27–31]. This technique allows for the quantification of their geometric features and spatial relationships. Using Generalized Procrustes superimposition (GPA) of landmarks configurations [32], GM allows for a quantitative separation of size and 3D shape. Size is measured as centroid size (the summed squared distances between the centroid and each of the landmarks of a given configuration). Shape contains all features of the landmark configurations that are invariant to scale, position and orientation [27,31] and can be quantified through the Procrustes shape coordinates of landmark configurations after GPA. While centroid size is a 1-dimensional variable, shape is intrinsically multidimensional (3D shape coordinates) and requires multivariate statistics for its analysis [27,33]. Thus, the landmark configurations appear as points in a multivariate shape space and the distances between these points in shape space correspond directly to the distances between all the homologous landmarks after GPA – also known as Procrustes distances [28,34]. Therefore, any statistical analysis in GM can directly be visualized as thin-plate splines transformations of 3D landmark configurations for graphic interpretation [27,29].

We designed two templates of digitization to measure the rib cage and the thoracic spine morphology of the subjects composing our sample. The 24 virtual models were digitized using Viewbox 4 software (www.dhal.com). The template for the ribs was developed by Bastir et al. [18,20] and consists of 402 landmarks and curve semilandmarks distributed on ribs 1 to 10 (Fig. 1). Because CT-scanning was carried out to include the skeletal thorax to the level of the diaphragm, in many cases the 11th and 12th ribs were not available for measurement. In consequence, we only took landmark coordinates on the non-floating ribs [20,35]. The landmarks (140 in total) are located on the upper and lowermost parts of each rib head, on the most anterior part of the intraarticular crests, on the most lateral part of the tubercles, on the inferior part of the costal angles, on the upper and lowermost parts of each sternal rib end and on the superior and inferior parts of the manubrium. In addition, 13 curve semilandmarks were placed along the inferior shaft of each rib, which means a total of 260 semilandmarks.

The thoracic spine template was designed by González-Ruiz [36] and is composed of a total of 240 landmarks and curve semilandmarks distributed on the 12 thoracic vertebrae (Fig. 2). The landmarks (120 in total) are located on each vertebra on the most anterior part of the superior and inferior costal facets, the most lateral parts of both transverse processes, the most anterior part of the spinous process (superior view) where it meets the most posterior point of the vertebral foramen, the most posterior part of the spinous process and the most inferior and lateral part of both laminae. Also, five curve semilandmarks (120 in total) were placed along both the upper and lower margins of the intervertebral surfaces (on the annular epiphysis) of each vertebra.

While landmarks are homologous points easily identifiable in all the specimens, semilandmarks are not anatomically homolo-

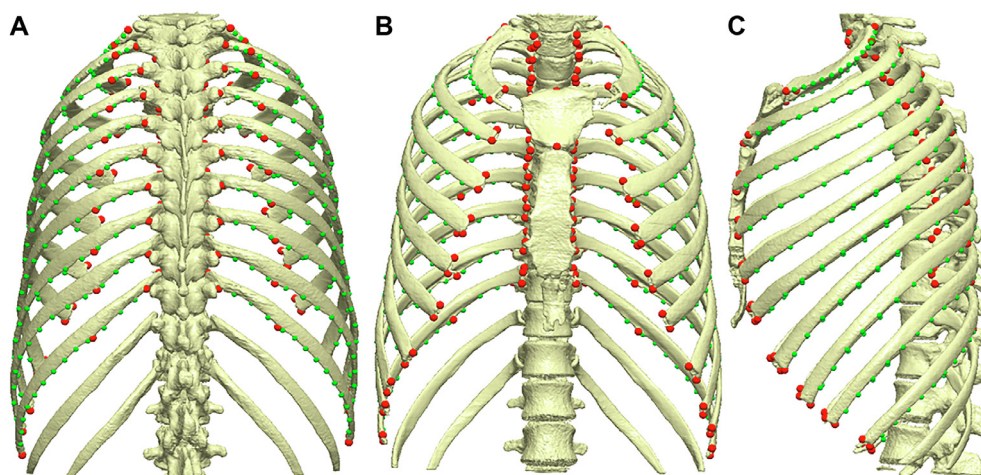


Fig. 1. Thorax digitization template in (A) posterior view, (B) anterior view, and (C) left lateral view. Red: landmarks; Green: curve semilandmarks.

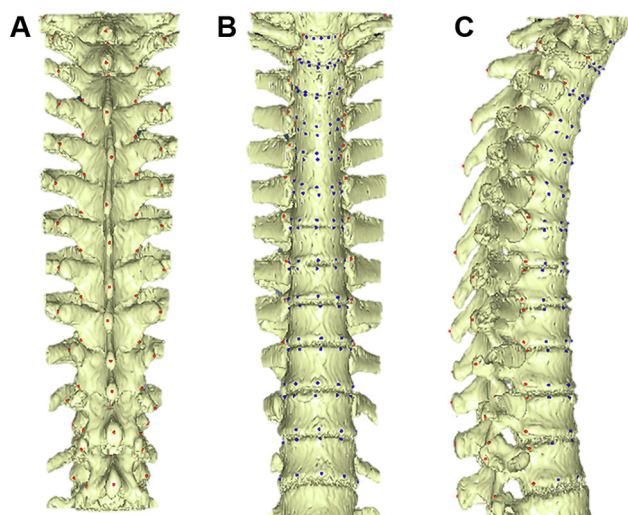


Fig. 2. Thoracic spine template in (A) anterior view, (B) right lateral view, and (C) posterior view. Red: landmarks; Blue: curve semilandmarks.

gous points and their localization in the specimens is uncertain [37,38]. In order to minimize this uncertainty in terms of their location when placing the semilandmarks along the curve, they were allowed to slide along tangent lines to their corresponding curves with respect to a reference configuration (template), as described by Gunz et al. [37]. By means of this sliding process, we find the optimal location for the semilandmarks (mathematical homology) with the morphometric difference (quantified as bending energy) between each specimen and the digitization template being minimal [37,38].

Data analysis

First, Procrustes shape coordinates were analysed by means of Principal components analysis (PCA) [31]. This analysis does not allow the hypothesis to be tested statistically, but it is useful to explore overall patterns of biological shape variation in the OI sample.

Second, in order to explore the quantitative relationship between the rib cage and thoracic spine shape and the respiratory function of OI patients [14], and hence our hypothesis, we regressed our shape data (both of the spine and the ribcage separately) on the respiratory variables FVC, FEV1, FVC % predicted, and FEV1 % predicted [39]. These regressions were carried out from two different approaches: (1) we first carried out two PCA separately for the samples of the ribs and the thoracic spines in order to reduce the number of variables [31] and we regressed the resulting PC scores on respiratory function (FVC, FEV1, FVC % predicted, and FEV1 % predicted) in a statistical shape space (PCA tangent space) composed of a subset of PCs accounting for at least for 95% of total variance. (2) We secondly regressed Procrustes shape coordinates (3D shape data collecting rib deformations and scoliosis) on respiratory function (FVC, FEV1, FVC % predicted, and FEV1 % predicted) in full shape space (100% of total variance). These regression analyses were applied to the full sample consisting of the OI-patients and the control group and corrected for sexual dimorphism (pooled-within sex) and health condition (OI vs. control healthy sample). We corrected these differences because function is clearly related to sexual dimorphism [19,22,35] and we wanted to identify non-sex specific features related to mal-function. A final regression analysis of the OI sample only (pooled

within sex) was applied to identify those anatomical features that lead to reduced respiratory capacities in OI-patients. Principal component analyses and regressions were performed in MorphoJ 1.06d [40], and all visualizations were produced using landmark-driven thin-plate spline transformations of 3D surface meshes by Evan toolkit (<http://www.evan-society.org/>). Continuous variables were presented as median and interquartile range. Difference between groups was performed with the Mann-Whitney test. Two-sided $p < 0.05$ was considered statistically significant. Statistical analyses were performed using SPSS v.23 software (SPSS Inc., Chicago, IL, USA).

Results

Results of the principal component analyses of the ribs and the thoracic spine are shown in Tables 3 and 4 respectively. We found that the 95% of the total variance required to carry out the regression analyses on statistical shape space was yielded by 11 PCs in the rib sample and by 9 PCs in the spine sample. Subsequent regression analyses on the full sample (OI + control subjects) showed a significant relation between rib shape and FEV1, FVC and FVC % pred (Table 5). On the contrary, no statistically significant relation was found between thoracic spine shape and FEV1, FEV1 % pred, FVC or FVC % pred on the full sample.

Results of the principal component analysis of the thorax of the OI sample are shown in Figs. 3 and 4. We can see, respectively, how OI-patients are distributed in shape space and the associated shape variations that reflect complex patterns of 3D rib-deformations (curvatures in the transversal planes) and variations in the declination both in sagittal and coronal planes of the thoracic cage, which also generates scoliosis and kyphosis.

Subsequent regression analyses on OI patients confirmed significant relations between ribs and respiratory function (Fig. 5A, Table 6), with Fig. 5B and C showing the associated shape changes. Thus, lower FEV1 and FVC values are observed in OI patients

Table 3

Principal component analysis of the ribs (11 principal components account for 95% of total variance).

PC	Eigenvalues	% Variance	Cumulative %
1	0.00742277	42.922	42.922
2	0.00276568	15.993	58.915
3	0.00234285	13.548	72.463
4	0.00142597	8.246	80.708
5	0.00069614	4.025	84.734
6	0.00050447	2.917	87.651
7	0.00041652	2.409	90.059
8	0.0003123	1.806	91.865
9	0.00025462	1.472	93.338
10	0.00019087	1.104	94.441
11	0.00016462	0.952	95.393

Table 4

Principal component analysis of the thoracic spine (9 principal components accounted for 95% of total variance).

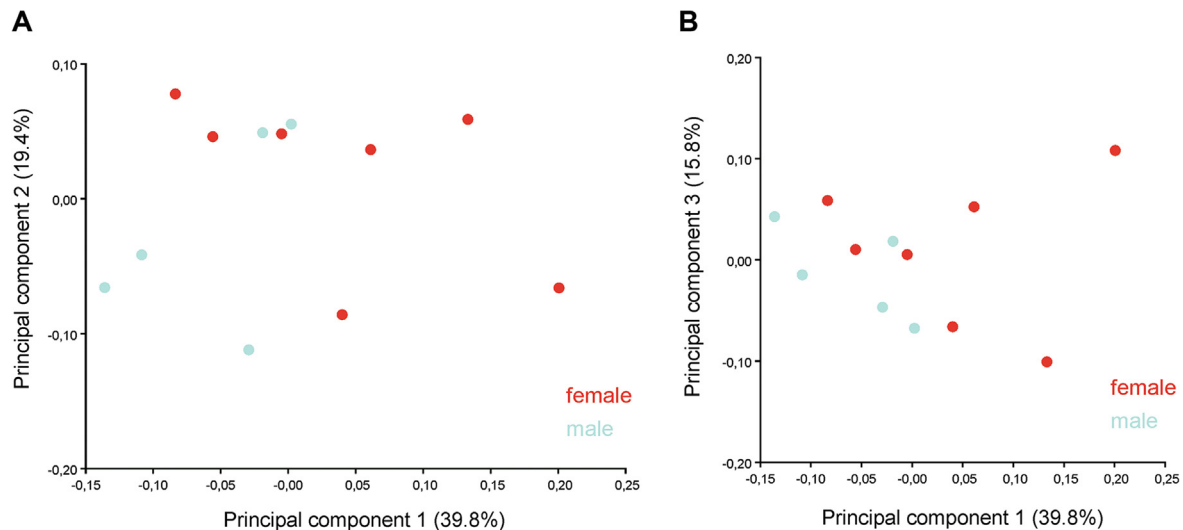
PC	Eigenvalues	% Variance	Cumulative %
1	0.00607063	44.958	44.958
2	0.0030622	22.678	67.637
3	0.00143914	10.658	78.295
4	0.00090092	6.672	84.967
5	0.00057603	4.266	89.233
6	0.00030397	2.251	91.484
7	0.00022045	1.633	93.117
8	0.00015541	1.151	94.268
9	0.00014872	1.101	95.369

Table 5

Multivariate regressions of ribs and thoracic spine shape on respiratory function in Osteogenesis Imperfecta patients + control healthy subjects (pooled within sex and group).

	Full shape ribs		Full shape thoracic spine	
	% explained variance	Significance	% explained variance	Significance
FEV1	16.5	0.001	6.8	ns
FEV1% pred	4.4	ns	5.7	ns
FVC	19.8	0.001	10.2	ns
FVC% pred	9.3	0.043	6.9	ns

ns: non-significant; FVC: forced vital capacity; FEV1: forced expiratory volume in 1 s, FVC% pred: forced vital capacity expressed as percentage of predicted value; FEV1% pred: forced expiratory volume in 1 s expressed as percentage of predicted value.

**Fig. 3.** Principal component analysis of the thoracic cages of the OI sample. (A) Scatterplots of PC1 vs. PC2, and (B) PC1 vs. PC3.

(males and females) with more horizontally aligned ribs, a greater antero-posterior depth due to extreme transverse curve at rib angles and a strong spine invagination, greater asymmetry, and a vertically shorter, thoraco-lumbar spine, which is relatively straight at levels 1–8 and shows a marked kyphosis in the thoraco-lumbar transition.

Discussion

Here we present the first 3D geometric morphometrics study of the thorax of OI patients. The correlation between impaired respiratory function and thoracic spine deformity in OI has been previously investigated. Widmann et al. [41] demonstrated a correlation between pulmonary function variables and the scoliosis angle but did not find any correlation between kyphosis, chest wall deformities and FVC, while Wekre et al. [42] demonstrated correlations between spirometry indexes corrected with arm span height and spinal deformities reflected in spine deformity index. In this context, Norimatsu et al. [43] suggested that respiratory dysfunction may be secondary to progressive spinal deformity based on serial pulmonary function testing in five patients with OI and a 14-year follow-up of FVC. On the other side, Falvo et al. [44] concluded that there are no significant differences in the results of pulmonary function testing in patients with OI and associated kyphoscoliosis and the general population with kyphoscoliosis without OI.

In addition, Lo Mauro et al. [14] noted that patients with severe OI are characterized by *pectus carinatum* and it has been postulated that this altered geometry causes considerable consequences in terms of volume variations of the chest wall compartments during breathing, since the deformed ribcage alters the normal action of

the intercostal muscles and requires the diaphragm to compensate for the reduced contribution to tidal volume. However, rather than the chest wall, we have analyzed the skeletal thorax of OI patients by means of 3D geometric morphometrics. Our regression analyses showed a significant relationship between ribs shape and FEV1, FVC and FVC % pred, and no statistically significant relation between thoracic spine shape and FEV1, FVC, FEV1 % pred, and FVC % pred; as a consequence, our results support the hypothesis that ribs are more relevant for respiratory function in OI patients than the scoliosis, as suggested by Lo Mauro et al. [14].

The FVC denomination as vital capacity is not capricious [45]. In fact, it is well known that reduced levels of ventilatory function, measured as FVC or FEV1, are associated with higher all-cause mortality rates, and therefore shorter survival in the general population [45–47]. Both for all-cause mortality and more specifically for circulatory disease mortality, FVC and FEV1 are as strongly predictive as body mass index and more strongly predictive than systolic blood pressure, even among lifelong non-smokers [46]. Although no specific information about the prognostic value of spirometric measurements in patients with OI is available, pulmonary complications are a significant cause for morbidity and mortality in these patients. Moreover, in a large cohort of individuals with OI enrolled in a multicenter, observational study, patients with more severe disease had lowest values of FVC and FEV1 [48]. These findings are compatible with a restrictive ventilatory disorder, which induces chronic respiratory symptoms and results in severe thoracic insufficiency syndrome and early death [49]. In turn, other circumstances have been implicated in the mortality excess reported in patients with a restrictive disorder, such as a higher incidence of cardiovascular disease, pulmonary hypertension, lung cancer, systemic inflammation and diabetes, among other [45].

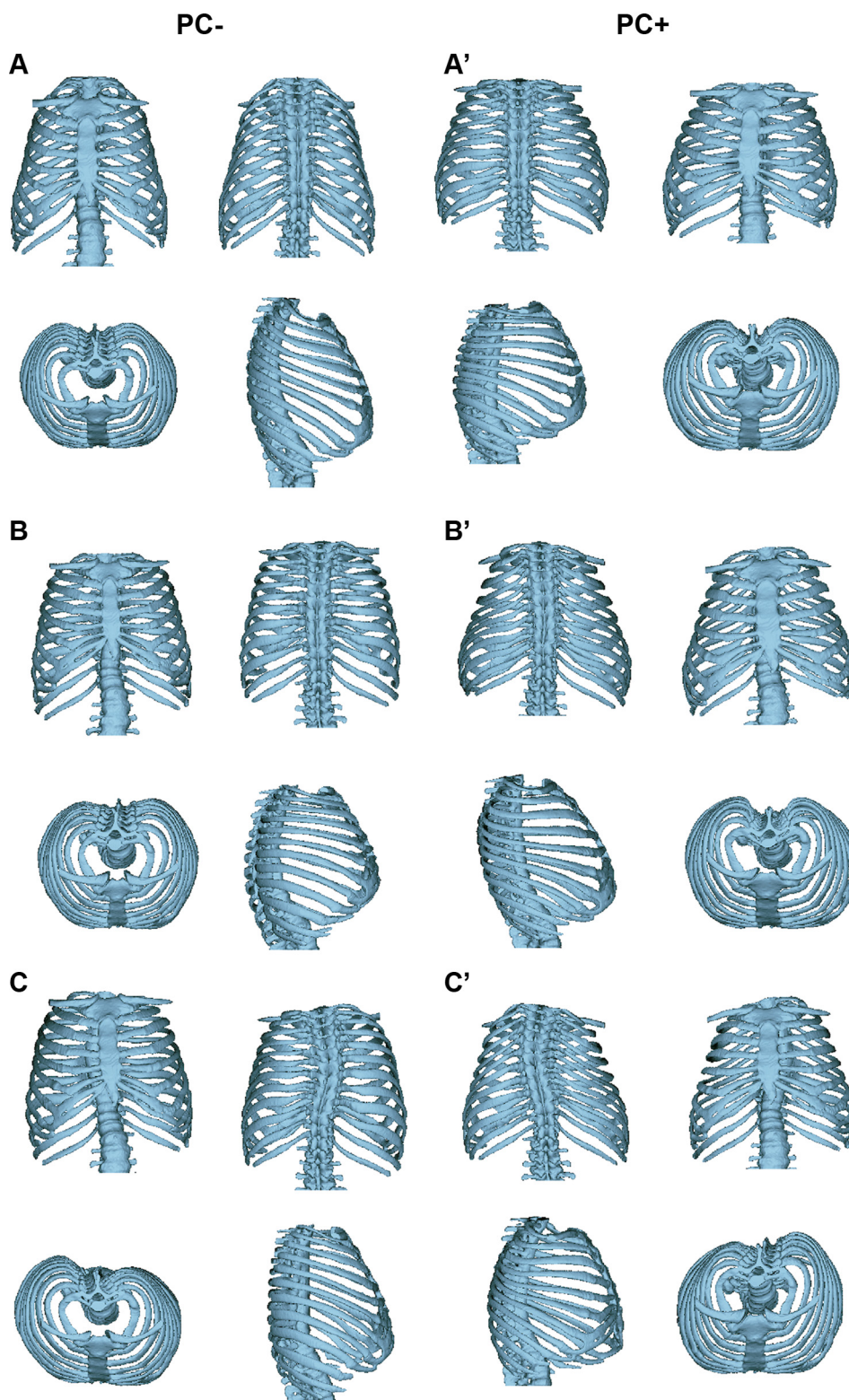


Fig. 4. Shapes associated to the PCA of the thoracic cages of the OI sample. Left column: shape associated with negative PC scores, Right column: shapes associated with positive PC scores. (A) Negative PC1 scores show tall ribcages, with downwards inclined ribs, flatter ribcages. (A') Positive PC1 scores show vertically shorter ribcages, horizontal ribs, invaginated spines, deep rib cages. (B) Negative PC2 scores show ribcages are more barrel-shaped due to more horizontally aligned proximal ribs. (B') Positive PC2 scores show ribcages are caudally much wider than cranially due to proximal rib declination, also thoracic spine strongly invaginated. (C) Negative PC3 scores show asymmetric features: barrel-shaped ribcage with scoliosis towards the right, thoracic spine relatively straight in the sagittal plane and vertically tall. (C') Positive PC3 scores show asymmetric features: caudally diverging ribcage with scoliosis towards the left, thoracic spine strongly kyphotic and vertically short.

As related before, different researchers have analyzed the influence of spine, ribs and morphology of the thorax (i.e. *pectus carinatum*) of OI patients on respiratory function but, to our knowledge,

our study is the first one to present the complete internal skeletal anatomy as a whole (ribs, spine and their deformities) and reveals the relationship between rib shape and respiratory function. In this

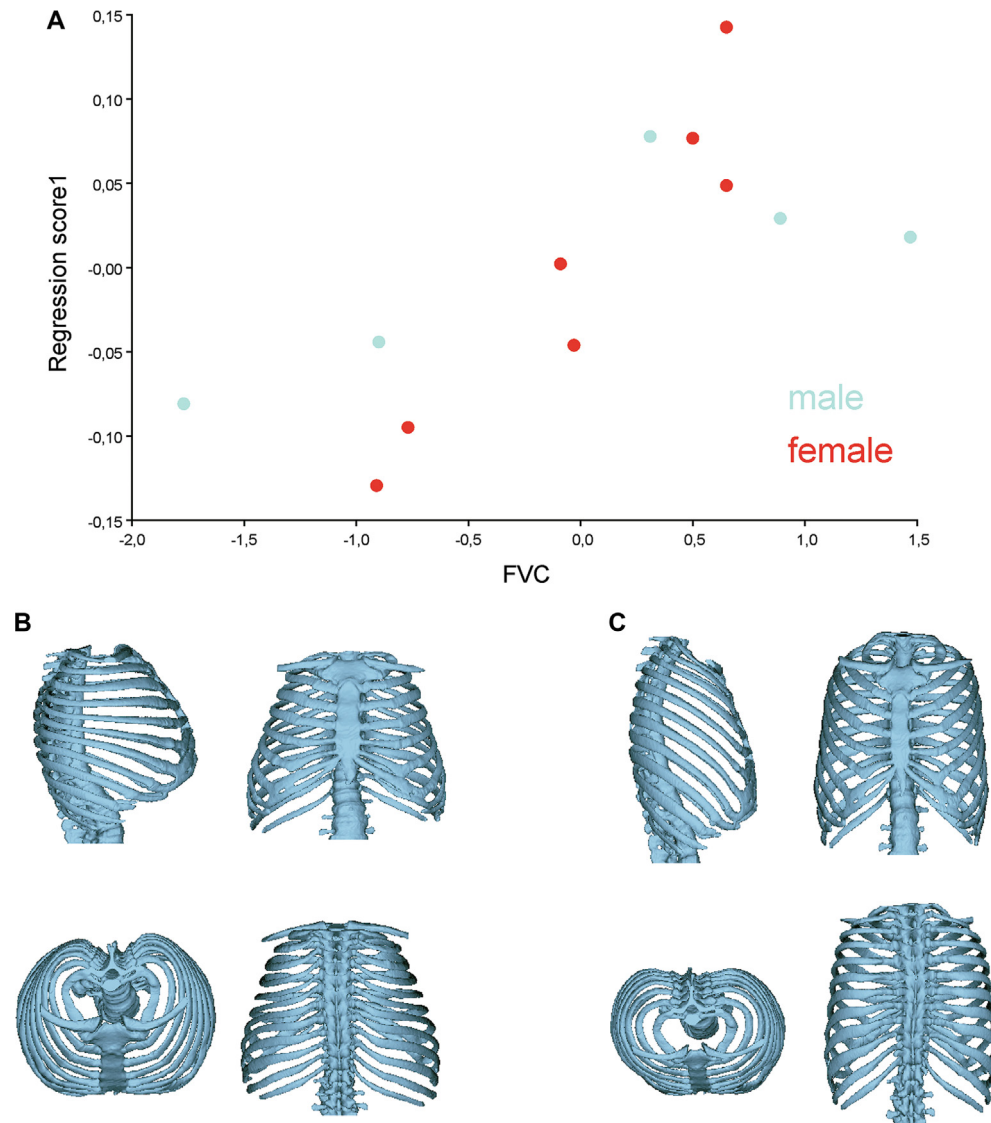


Fig. 5. Regression analysis of the thoracic cages of the OI-patients sample (pooled within sex) indicating the shape features that are related to respiratory function. (A) Regression of shape versus FVC; (B) Shape features related to lower FVC; and (C) shape features related to higher FVC values. Note the differences in the orientation of the ribs, the relative height of the thoracic spine and the complex patterns of 3D curvatures.

Table 6

Multivariate regression of rib shape on respiratory function in Osteogenesis Imperfecta patients (pooled within sex).

	Full shape ribs		95% rib shape variance	
	% explained variance	Significance	% explained variance	Significance
FEV1	17.1	0.055	17.6	0.047
FEV1% pred	6.8	ns	6.4	ns
FVC	18	0.040	18.4	0.043
FVC% pred	7.1	ns	6.8	ns

ns: non-significant; FVC: forced vital capacity; FEV1: forced expiratory volume in 1 s, FVC% pred: forced vital capacity expressed as percentage of predicted value; FEV1% pred: forced expiratory volume in 1 s expressed as percentage of predicted value.

context, our results showed that worse respiratory function in OI patients is related to an anatomic configuration characterized by more horizontally aligned ribs, a greater antero-posterior depth due to extreme transverse curve at rib angles and a strong spine invagination, greater asymmetry, and a vertically short, thoraco-lumbar spine, which is relatively straight in the superior part and shows a marked kyphosis in the thoraco-lumbar transition being scoliosis less evident in this 3D geometric morphometrics model.

Further research by means of magnetic resonance imaging may be needed in order to analyze the possible shape changes of the intercostal muscles as a consequence of the related rib cage deformities we found.

Results obtained on the anatomic OI model are of special importance as OI is a progressive disease. Our results suggest that OI patients need early therapeutic actions in order to retard and/or avoid the appearance of the thorax deformities we described

(Fig. 5), because subjects with severe OI present, since childhood, a rapid and shallow breathing pattern characterized by significantly higher breathing frequency [17], being the respiratory complication the main cause of death in OI also during childhood [6–8]. In this context, many studies have found that bisphosphonate therapy for children with OI, when started early in life, leads to increased bone density, decreased fracture rate, recovery of the shape of vertebral bodies [50,51] and preservation of vertebral shape [52]. Published data suggest that bisphosphonate treatment decreases the rate of progression of scoliosis in children with OI when therapy starts before the age of six years [53], but does not modify the prevalence of moderate to severe scoliosis at maturity [54]. It should be noted that all our patients were in treatment with bisphosphonates. Together with this, Lo Mauro et al. [17] suggested that specific physiotherapy targeted to the rib cage muscles may be started in early childhood in severe OI to try to delay or reduce the effects of the progressively reduced action of these muscles. Furthermore, we suggest to combine the physiotherapy targeted to the ribcage muscles proposed by Lo Mauro et al. [17] with specific surgery and specific orthopedic care [55] in order to avoid the appearance of the rib cage deformities we present. Finally, we want to highlight the potential clinical implication of our results. The identification that alterations in the ventilatory mechanics of patients with OI is more depend on rib cage dynamics than on the dorsal spine raises the possibility of developing therapeutic interventions aimed to promote thoracic cage mobility, which a priori it is more feasible than modify the structure of vertebral bodies.

Our study presents some limitations: firstly, the relatively low number of patients. It should be taken into consideration here that OI has been classified as a rare disease. In addition, our study was carried out by means of CT scans, with its associated radiation exposure. Nevertheless, participation of all OI subjects was voluntary after being advised about the radiation exposure and CT studies were carried out in order to control the skeletal basis of the evolution of their disease.

Conclusions

Therefore, despite the above-mentioned limitations, we consider the results of this translational study may have important consequences on future clinical functional evaluation and should be completed by further studies that include a larger number of patients. We also believe the results presented here will serve for a better management of OI patients that may include a new clinical approach based on control, avoiding and correction of the thorax deformities for obtaining a better respiratory function in these patients. Also, further research will be necessary in order to compare the pulmonary function of OI patients after correction of their thorax deformities.

Compliance with ethics requirements

All procedures followed were in accordance with the ethical standards of the responsible committee on human experimentation (institutional and national) and with the Helsinki Declaration of 1975, as revised in 2008 (5). Informed consent was obtained from all patients for being included in the study.

Declaration of Competing Interest

The authors declare that they have no known competing financial interests or personal relationships that could have appeared to influence the work reported in this paper.

Acknowledgments

This project was funded by grants of the Fundacion Eresa (grant number: BF14_005), the Ministry of Economy, Industry and Competitiveness (grant number: CGL2015-63648-P), the Care4Brittlebones Foundation (grant number: OTR2016-15543INVES), and the University of Valencia (grant number: UV-INV_AE18-773873).

We would like to thank the Fundacion Ahuce, the Care4Brittlebones Foundation, and Ms. Julia Piniella, from Fundacion Ahuce, for her assistance in the different phases of this research work. We would also like to thank all the patients who voluntarily agreed to participate in this study.

References

- [1] Marini JC, Blissett AR. New genes in bone development: what's new in osteogenesis imperfecta. *J Clin Endocrinol Metab* 2013;98:3095–103.
- [2] Byers PH, Steiner RD. Osteogenesis imperfecta. *Annu Rev Med* 1992;43:269–82.
- [3] Rauch F, Glorieux FH. Osteogenesis imperfecta. *Lancet* 2004;363:1377–85.
- [4] Sillence DO, Senn A, Danks DM. Genetic heterogeneity in osteogenesis imperfecta. *J Med Genet* 1979;16:101–16.
- [5] Sillence DO, Barlow KK, Cole WG, Dietrich S, Garber AP, Rimoin DL. Osteogenesis imperfecta type III. Delineation of the phenotype with reference to genetic heterogeneity. *Am J Med Genet* 1986;23:821–32.
- [6] McAllion SJ, Paterson CR. Causes of death in osteogenesis imperfecta. *J Clin Pathol* 1996;49:627–30.
- [7] Paterson CR, Ogston SA, Henry RM. Life expectancy in osteogenesis imperfecta. *BMJ* 1996;312:351.
- [8] Singer RB, Ogston SA, Paterson CR. Mortality in various types of osteogenesis imperfecta. *J Inher Med* 2001;33:216–20.
- [9] Sinikumpu JJ, Ojaniemi M, Lehenkari P, Serlo W. Severe osteogenesis imperfecta type-III and its challenging treatment in newborn and preschool children. *A System Rev Injury* 2015;46:1440–6.
- [10] Wallace MJ, Kruse RW, Shah SA. The spine in patients with osteogenesis imperfecta. *J Am Acad Orthop Surg* 2017;25:100–9.
- [11] Antoniazzi F, Mottes M, Franchini P, Brunelli PC, Tatò L. Osteogenesis imperfecta: practical treatment guidelines. *Paediatr Drugs* 2000;2:465–88.
- [12] Benson DR, Donaldson DH, Millar EA. The spine in osteogenesis imperfecta. *J Bone Joint Surg Am* 1978;60:925–9.
- [13] Paterson CR, McAllion SJ, Shaw JW. Clinical and radiological features of osteogenesis imperfecta type IVA. *Acta Paediatr Scand* 1987;76:548–52.
- [14] LoMauro A, Pochintesta S, Romei M, D'Angelo MG, Pedotti A, Turconi AC, et al. Rib cage deformities alter respiratory muscle action and chest wall function in patients with severe osteogenesis imperfecta. *PLoS ONE* 2012;7:e35965.
- [15] Van Dijk FS, Sillence DO. Osteogenesis imperfecta: Clinical diagnosis, nomenclature and severity assessment. *Am J Med Genet A* 2014;164:1470–81.
- [16] Al Kaissi A, Ben Chehida F, Grill F, Ganger R. Progressive collapse of the thoracic cage. *Am J Med* 2016;129:e1–4.
- [17] LoMauro A, Franchini P, Pochintesta S, Romei M, D'Angelo MG, Aliverti A. Ribcage deformity and the altered breathing pattern in children with osteogenesis imperfecta. *Pediatr Pulmonol* 2018;53:964–72.
- [18] Bastir M, García Martínez D, Recheis W, Barash A, Coquerelle M, Ríos L, et al. Differential growth and development of the upper and lower human thorax. *PLoS ONE* 2013;8:e75128.
- [19] García-Martínez D, Torres-Tamayo N, Torres-Sánchez I, García-Río F, Bastir M. Morphological and functional implications of sexual dimorphism in the human skeletal thorax. *Am J Phys Anthropol* 2016;161:467–77.
- [20] Bastir M, García-Martínez D, Torres-Tamayo N, Sanchis-Gimeno JA, O'Higgins P, Utrilla C, et al. In vivo 3d analysis of thoracic kinematics: Changes in size and shape during breathing and their implications for respiratory function in recent humans and fossil hominins. *Anat Rec* 2017;300:255–64.
- [21] García-Martínez D, Nalla S, Ferreira MT, Guichón RA, D'Angelo Del Campo MD, Bastir M. Eco-geographic adaptations in the human ribcage throughout a 3D geometric morphometric approach. *Am J Phys Anthropol* 2018;166:323–36.
- [22] Torres-Tamayo N, García-Martínez D, Lois Zolniski S, Torres-Sánchez I, García-Río F, Bastir M. 3D analysis of sexual dimorphism in size, shape and breathing kinematics of human lungs. *J Anat* 2018;232:227–37.
- [23] García-Río F, Calle M, Burgos F, Casan P, Del Campo F, Spirometry Galdiz JB, et al. Society of Pulmonology and Thoracic Surgery (SEPAR). Spanish Society of Pulmonology and Thoracic Surgery (SEPAR). *Arch Bronconeumol* 2013;49:388–401.
- [24] European Respiratory Society (ERS). Global Lung Function Initiative. <https://www.ers-education.org/guidelines/global-lung-function-initiative/spirometry-tools.aspx>; 2012 [accessed 25 June 2019].
- [25] Calzado A, Geleijns J. Computed tomography. Evolution, technical principles and applications. *Rev Fis Med* 2010;11:163–80.
- [26] Lorensen WE, Cline HE. Marching cubes: a high resolution 3D surface construction algorithm. *ACM SIGGRAPH Comput Graph* 1987;21:163–9.
- [27] Bookstein FL. Morphometric tools for landmark data. Cambridge: Cambridge University Press; 1991.

- [28] Rohlf FJ, Marcus LF. A revolution in morphometrics. *Tree* 1993;8:129–32.
- [29] O'Higgins P. The study of morphological variation in the hominid fossil record: biology, landmarks and geometry. *J Anat* 2000;197:103–20.
- [30] Mitteroecker P, Gunz P. Advances in geometric morphometrics. *Evol Biol* 2009;36:235–47.
- [31] Zelditch ML, Swiderski DL, Sheets HD, Fink WL. Geometric morphometrics for biologists: a primer. San Diego: Elsevier Academic Press; 2012.
- [32] Gower JC. Generalized procrustes analysis. *Psychometrika* 1975;40:33–51.
- [33] Bookstein FL. Combining the tools of geometric morphometrics. In: Marcus LF, editor. *Advances in morphometrics*. New York: Plenum Press; 1996. p. 131–51.
- [34] Rohlf FJ. Morphometric spaces, shape components and the effects of linear transformations. In: Marcus LF, editor. *Advances in morphometrics*. New York: Plenum Press; 1996. p. 117–28.
- [35] García-Martínez D, Bastir M, Torres-Tamayo N, O'Higgins P, Torres-Sánchez I, García-Río F, et al. Three-dimensional analysis of sexual dimorphism in ribcage kinematics of modern humans. *Am J Phys Anthropol* 2019;169:348–55.
- [36] González-Ruiz JM. La Morfometría Geométrica como herramienta aplicada al estudio de la escoliosis en pacientes con osteogénesis imperfecta [Master's dissertation]. Madrid, Spain: Autonomous University of Madrid; 2018.
- [37] Gunz P, Mitteroecker P, Bookstein FL. Semilandmarks in three dimensions. In: Slice DE, editor. *Modern morphometrics in physical anthropology*. New York: Kluwer Academic/Plenum Publishers; 2005. p. 73–98.
- [38] Gunz P, Mitteroecker P. Semilandmarks: a method for quantifying curves and surfaces. *Hystrix It J Mammal* 2013;24:103–9.
- [39] West JB. *Respiratory physiology: The essentials*. 9th ed. Philadelphia: Wolters Kluwer, Lippincott Williams & Wilkins; 2012.
- [40] Klingenberg CP. MorphoJ: an integrated software package for geometric morphometrics. *Mol Ecol Resour* 2011;11:353–7.
- [41] Widmann RF, Bitan FD, Laplaza FJ, Burke SW, DiMaio MF, Schneider R. Spinal deformity, pulmonary compromise, and quality of life in osteogenesis imperfecta. *Spine* 1999;24:1673–8.
- [42] Wekre LL, Kjensli A, Aasand K, Falch JA, Eriksen EF. Spinal deformities and lung function in adults with osteogenesis imperfecta. *Clin Respir J* 2014;8:437–43.
- [43] Norimatsu H, Mayuzumi T, Takahashi H. The development of the spinal deformities in osteogenesis imperfecta. *Clin Orthop* 1982;162:20–5.
- [44] Falvo KA, Klain DB, Krauss AN, Root L, Auld PA. Pulmonary function studies in osteogenesis imperfecta. *Am Rev Respir Dis* 1973;108:1258–60.
- [45] Godfrey MS, Jankowich MD. The vital capacity is vital: epidemiology and clinical significance of the restrictive spirometry pattern. *Chest* 2016;149:238–51.
- [46] Gupta RP, Strachan DP. Ventilatory function as a predictor of mortality in lifelong non-smokers: evidence from large British cohort studies. *BMJ Open* 2017;7:e015381.
- [47] Magnussen C, Ojeda FM, Rzaeva N, Zeller T, Sinning CR, Pfeiffer N, et al. FEV1 and FVC predict all-cause mortality independent of cardiac function - Results from the population-based Gutenberg Health Study. *Int J Cardiol* 2017;234:64–8.
- [48] Tam A, Chen S, Schauer E, Grafe I, Bandi V, Shapiro JR, et al. A multicenter study to evaluate pulmonary function in osteogenesis imperfecta. *Clin Genet* 2018;94:502–11.
- [49] Ramírez N, Cornier AS, Campbell Jr RM, Carlo S, Arroyo S, Romeu J. Natural history of thoracic insufficiency syndrome: a spondylothoracic dysplasia perspective. *J Bone Joint Surg Am* 2007;89:2663–75.
- [50] Semler O, Beccard R, Palmisano D, Demant A, Fricke O, Schoenau E, et al. Reshaping of vertebrae during treatment with neridronate or pamidronate in children with osteogenesis imperfecta. *Horm Res Paediatr* 2011;76:321–7.
- [51] Palomo T, Fassier F, Ouellet J, Sato A, Montpetit K, Glorieux FH, et al. Intravenous bisphosphonate therapy of young children with osteogenesis imperfecta: skeletal findings during follow up throughout the growing years. *J Bone Miner Res* 2015;30:2150–7.
- [52] Cristofaro RL, Hoek KJ, Bonnett CA, Brown JC. Operative treatment of spine deformity in osteogenesis imperfecta. *Clin Orthop* 1979;139:40–8.
- [53] Anissipour AK, Hammerberg KW, Caudill A, Kostiuik T, Tarima S, Zhao HS, et al. Behavior of scoliosis during growth in children with osteogenesis imperfecta. *J Bone Joint Surg Am* 2014;96:237–43.
- [54] Sato A, Ouellet J, Muneta T, Glorieux FH, Rauch F. Scoliosis in osteogenesis imperfecta caused by COL1A1/COL1A2 mutations – genotype-phenotype correlations and effect of bisphosphonate treatment. *Bone* 2016;86:53–7.
- [55] Franzone JM, Shah SA, Wallace MJ, Kruse RW. Osteogenesis imperfecta: A pediatric orthopedic perspective. *Orthop Clin North Am* 2019;50:193–209.